Asymmetric transmission of terahertz waves using polar dielectrics

Andriy E. Serebryannikov,[1,2,*] Ekmel Ozbay,[1] and Shunji Nojima[3]

[1]*Nanotechnology Research Center, Bilkent University, 06800 Ankara, Turkey*
[2]*Hamburg University of Technology, E-3, D-21071 Hamburg, Germany*
[3]*Department of Nanosystem Science, Graduate School of Nanobioscience, Yokohama City University, 22-2 Seto, Kanazawa Ku, Yokohama, Kanagawa 236-0027, Japan*
[*]*serebryannikov@tu-harburg.de*

Abstract: Asymmetric wave transmission is a Lorentz reciprocal phenomenon, which can appear in the structures with broken symmetry. It may enable high forward-to-backward transmittance contrast, while transmission for one of the two opposite incidence directions is blocked. In this paper, it is demonstrated that ultrawideband, high-contrast asymmetric wave transmission can be obtained at terahertz frequencies in the topologically simple, i.e., one- or two-layer nonsymmetric gratings, which are entirely or partially made of a polar dielectric working in the ultralow-ε regime inspired by phonon-photon coupling. A variety of polar dielectrics with different characteristics can be used that gives one a big freedom concerning design. Simple criteria for estimating possible usefulness of a certain polar dielectric are suggested. Contrasts exceeding 80dB can be easily achieved without a special parameter adjustment. Stacking a high-ε corrugated layer with a noncorrugated layer made of a polar dielectric, one can enhance transmission in the unidirectional regime. At large and intermediate angles of incidence, a better performance can be obtained owing to the common effect of nonsymmetric diffractions and directional selectivity, which is connected with the dispersion of the ultralow-ε material. At normal incidence, strong asymmetry in transmission may occur in the studied structures as a purely diffraction effect.

OCIS codes: (050.1970) Diffractive optics; (050.1960) Diffraction theory; (120.7000) Transmission; (160.4670) Optical materials; (999.9999) Terahertz waves.

References and links

1. M. J. Lockyear, A. P. Hibbins, K. R. White, and J. R. Sambles, "One-way diffraction grating," Phys. Rev. E Stat. Nonlinear Soft Matter Phys. **74**(5), 056611 (2006).
2. A. E. Serebryannikov and E. Ozbay, "Unidirectional transmission in non-symmetric gratings containing metallic layers," Opt. Express **17**(16), 13335–13345 (2009).
3. A. E. Serebryannikov, A. O. Cakmak, and E. Ozbay, "Multichannel optical diode with unidirectional diffraction relevant total transmission," Opt. Express **20**(14), 14980–14990 (2012).
4. X.-B. Kang, W. Tan, Z.-S. Wang, Z.-G. Wang, and H. Cheng, "High-efficiency one-way transmission by one-dimensional photonic crystal with gratings on one side," Chin. Phys. Lett. **27**(7), 074204 (2010).
5. M. Stolarek, D. Yavorskiy, R. Kotyński, C. J. Zapata Rodríguez, J. Łusakowski, and T. Szoplik, "Asymmetric transmission of terahertz radiation through a double grating," Opt. Lett. **38**(6), 839–841 (2013).
6. A. Cicek, M. B. Yucel, O. A. Kaya, and B. Ulug, "Refraction-based photonic crystal diode," Opt. Lett. **37**(14), 2937–2939 (2012).
7. S. Cakmakyapan, A. E. Serebryannikov, H. Caglayan, and E. Ozbay, "Spoof-plasmon relevant one-way collimation and multiplexing at beaming from a slit in metallic grating," Opt. Express **20**(24), 26636–26648 (2012).
8. V. Liu, D. A. B. Miller, and S. Fan, "Ultra-compact photonic crystal waveguide spatial mode converter and its connection to the optical diode effect," Opt. Express **20**(27), 28388–28397 (2012).
9. D. Jalas, A. Petrov, M. Eich, W. Freude, S. Fan, Z. Yu, R. Baets, M. Popović, A. Melloni, J. D. Joannopoulos, M. Vanwolleghem, C. R. Doerr, and H. Renner, "What is - and what is not - an optical isolator," Nat. Photonics **7**(8), 579–582 (2013).
10. S. Xu, C. Qiu, and Z. Liu, "Acoustic transmission through asymmetric grating structures made of cylinders," J. Appl. Phys. **111**(9), 094505 (2012).

#202344 - $15.00 USD Received 2 Dec 2013; revised 20 Jan 2014; accepted 21 Jan 2014; published 3 Feb 2014

11. A. E. Serebryannikov and E. Ozbay, "One-way Rayleigh-Wood anomalies and tunable narrowband transmission in photonic crystal gratings with broken structural symmetry," Phys. Rev. A **87**(5), 053804 (2013).
12. A. E. Serebryannikov, K. B. Alici, T. Magath, A. O. Cakmak, and E. Ozbay, "Asymmetric Fabry-Perot-type transmission in photonic-crystal gratings with one-sided corrugations at a two-way coupling," Phys. Rev. A **86**(5), 053835 (2012).
13. M. Beruete, A. E. Serebryannikov, V. Torres, M. Navarro-Cia, and M. Sorolla, "Toward compact millimeter-wave diode in thin stacked-hole array assisted by a dielectric grating," Appl. Phys. Lett. **99**(15), 154101 (2011).
14. M. Mutlu, S. Cakmakyapan, A. E. Serebryannikov, and E. Ozbay, "One-way reciprocal spoof surface plasmons and relevant reversible diodelike beaming," Phys. Rev. B **87**(20), 205123 (2013).
15. W.-M. Ye, X.-D. Yuan, C. C. Guo, and C. Zen, "Unidirectional transmission in non-symmetric gratings made of isotropic material," Opt. Express **18**(8), 7590–7595 (2010).
16. A. E. Serebryannikov, T. Magath, K. Schuenemann, and O. Y. Vasylchenko, "Scattering of *s*-polarized plane waves by finite-thickness periodic structures made of ultralow-permittivity metamaterials," Phys. Rev. B **73**(11), 115111 (2006).
17. R. Singh, E. Plum, C. Menzel, C. Rockstuhl, A. K. Azad, R. A. Cheville, F. Lederer, W. Zhang, and N. I. Zheludev, "Terahertz metamaterial with asymmetric transmission," Phys. Rev. B **80**(15), 153104 (2009).
18. C. Wang, X.-L. Zhong, and Z.-Y. Li, "Linear and passive silicon optical isolator," Sci. Rep. **2**, 674 (2012).
19. J. H. Oh, H. W. Kim, P. S. Ma, H. M. Seung, and Y. Y. Kim, "Inverted bi-prism phononic crystals for one-sided elastic wave transmission applications," Appl. Phys. Lett. **100**(21), 213503 (2012).
20. E. Colak, A. E. Serebryannikov, A. O. Cakmak, and E. Ozbay, "Experimental study of broadband unidirectional splitting in photonic crystal gratings with broken structural symmetry," Appl. Phys. Lett. **102**(15), 151105 (2013).
21. A. E. Serebryannikov, E. Colak, A. O. Cakmak, and E. Ozbay, "Dispersion irrelevant wideband asymmetric transmission in dielectric photonic crystal gratings," Opt. Lett. **37**(23), 4844–4846 (2012).
22. B. T. Schwartz and R. Piestun, "Total external reflection from metamaterials with ultralow refractive index," J. Opt. Soc. Am. B **20**(12), 2448–2453 (2003).
23. R. W. Ziolkowski, "Propagation in and scattering from a matched metamaterial having a zero index of refraction," Phys. Rev. E Stat. Nonlinear Soft Matter Phys. **70**(4), 046608 (2004).
24. A. Alù, M. G. Silveirinha, A. Salandrino, and N. Engheta, "Epsilon-near-zero metamaterials and electromagnetic sources: Tailoring the radiation phase pattern," Phys. Rev. B **75**(15), 155410 (2007).
25. C. Kittel, *Introduction to Solid State Physics* (John Wiley, 2005).
26. M. M. Sigalas, C. M. Soukoulis, C. T. Chan, and K. M. Ho, "Electromagnetic-wave propagation through dispersive and absorptive photonic-band-gap materials," Phys. Rev. B Condens. Matter **49**(16), 11080–11087 (1994).
27. S. Foteinopoulou, M. Kafesaki, E. N. Economou, and C. M. Soukoulis, "Two-dimensional polaritonic photonic crystals as terahertz uniaxial metamaterials," Phys. Rev. B **84**(3), 035128 (2011).
28. K. C. Huang, M. L. Povinelli, and J. D. Joannopoulos, "Negative effective permeability in polaritonic photonic crystals," Appl. Phys. Lett. **85**(4), 543–545 (2004).
29. P. B. Catrysse and S. Fan, "Near-complete transmission through subwavelength hole arrays in phonon-polaritonic thin films," Phys. Rev. B **75**(7), 075422 (2007).
30. A. Rung, C. G. Ribbing, and M. Qiu, "Gap maps for triangular photonic crystals with a dispersive and absorbing component," Phys. Rev. B **72**(20), 205120 (2005).
31. S. Nojima, "Excitonic polaritons in one-dimensional photonic crystals," Phys. Rev. B **57**(4), R2057–R2060 (1998).
32. S. Nojima, "Photonic-crystal laser mediated by polaritons," Phys. Rev. B **61**(15), 9940–9943 (2000).
33. A. L. Yablonskii, E. A. Muljarov, N. A. Gippius, S. G. Tikhodeev, T. Fujita, and T. Ishihara, "Polariton effect in distributed feedback microcavities," J. Phys. Soc. Jpn. **70**(4), 1137–1144 (2001).
34. M. V. Erementchouk, L. I. Deych, and A. A. Lisyansky, "Spectral properties of exciton polaritons in one-dimensional resonant photonic crystals," Phys. Rev. B **73**(11), 115321 (2006).
35. S. Nojima, "Optical response of excitonic polaritons in photonic crystals," Phys. Rev. B **59**(8), 5662–5677 (1999).
36. T. Magath and A. E. Serebryannikov, "Fast iterative, coupled-integral-equation technique for inhomogeneous profiled and periodic slabs," J. Opt. Soc. Am. A **22**(11), 2405–2418 (2005).
37. E. D. Palik, ed., *Handbook of Optical Constants of Solids* (Academic, 1985).
38. P. Rodríguez-Ulibarri, M. Beruete, M. Navarro-Cia, and A. E. Serebryannikov, "Wideband unidirectional transmission with tunable sign-switchable refraction and deflection in nonsymmetric structures," Phys. Rev. B **88**(16), 165137 (2013).
39. R. Petit, ed., *Electromagnetic Theory of Gratings* (Springer, 1980).

1. Introduction

The interest to the asymmetric wave transmission has been growing over last years. This is a Lorentz reciprocal phenomenon, which manifests itself in strong difference between the forward and the backward transmission in the structures with broken spatial inversion symmetry for illumination directions that differ by 180 degrees, e.g., see [1–7]. In spite of that the functionalities associated with nonreciprocity, e.g., optical isolation cannot be obtained in

#202344 - $15.00 USD Received 2 Dec 2013; revised 20 Jan 2014; accepted 21 Jan 2014; published 3 Feb 2014

the frame of this mechanism, there are many others, which are realizable in various nonsymmetric structures made of linear, isotropic, passive materials [8,9]. In particular, the achievable operation regimes include single-beam deflection, diodelike transmission, and dual- and multibeam splitting [2,3,6,7]. In fact, asymmetric wave transmission is possible due to additional transmission channels, to which the incident wave is either coupled or uncoupled, depending on the illumination side. Such a channel may be created by involving a higher diffraction order or polarization state, which differs from that of the incident wave. Generally speaking, all these regimes can be explained in terms of one-way mode conversion. Various performances of nonsymmetric structures for asymmetric wave transmission in acoustic, microwave, and optical ranges have been suggested to this time. They include photonic crystal gratings [3,4,10–12], stacked hole arrays with one-side corrugations [13], metallic gratings with subwavelength slits [1,5,7,14], gratings that represent a one-fraction structure or a two-fraction structure obtained by either stacking two layers, one of which is corrugated, or embedding one single-fraction grating into another [2,15,16], and ultrathin structures based on subwavelength resonators that enable polarization manipulation [14,17]. Performance in terms of the asymmetry and band width can be especially strong when dispersion contributes to the resulting mechanism. Its potential has been demonstrated, for example, in photonic crystal gratings, where various regimes of wideband unidirectional transmission, i.e., those with transmission vanishing in a wide frequency range for one of the two opposite illumination directions have been obtained [3,10]. Moreover, inclining interfaces, as in photonic crystal prisms, allows one to further extend variety of the regimes that are achievable in the frame of the asymmetric wave transmission mechanism [6,18,19]. Unusual features relevant to the directional selectivity, which is inspired by the common effect of diffraction and dispersion, as in photonic crystal gratings, may include but are not restricted to one-way Rayleigh-Wood anomalies [11], unidirectional splitting [20], and reflection-free diodelike transmission [3]. On the other hand, it has been demonstrated in case of photonic crystal gratings that unidirectional transmission can be a purely diffraction effect, i.e., it can be achieved without the use of a peculiar dispersion [12,21]. Most of the known designs require structuring and/or assembling to obtain a proper configuration. Performances that can be easily fabricated and integrated with other components invoke materials whose properties could match the requirements to the asymmetric wave transmission without structuring. To this end, one should mention ultralow-ε (ε ranging from 0 to 1) and ultralow-index materials (refractive index ranging from 0 to 1) [22–24]. For such a material, equifrequency dispersion contours have a circular shape and are narrower than in air. Thus, they enable unidirectional transmission. Nonsymmetric gratings based on Drude materials have been proposed [2,16]. However, the range of $0 < \varepsilon < 1$ corresponds for most of metals to petahertz frequencies. At lower frequencies, Drude dispersion can be achieved by utilizing a wire medium, i.e., the structuring is still required [22].

If the terahertz frequency range is targeted, polar dielectrics can be suggested as a reasonable alternative, because they may show $0 < \varepsilon < 1$ in a wide frequency range [25]. The existence of such a range is connected with the coupling of photons with transverse optical phonons that leads to the appearance of polaritons [25]. The ranges of (ultra) high ε can appear in the frame of this mechanism for the same materials but at lower frequencies. In the last two decades, various periodic structures containing polar dielectrics, e.g., photonic crystals, metamaterials, hole arrays, and distributed microcavities have extensively been studied [26–33]. In particular, the periodicity relevant multiple excitonic polaritons and *polaritonic gaps* have been demonstrated in one-dimensional photonic crystals [31,34,35]. The polaritonic gap and strong dependence of permittivity on frequency occur also in non-structured polar dielectrics, where they have nothing to do with the periodicity. Both structured and nonstructured polar dielectrics can be useful for various applications related to light manipulation.

In this paper, we will study diffraction on nonsymmetric gratings, which are either partially or entirely made of polar dielectrics. Comparison of zero- and higher-order transmission and reflection at the corrugated-side illumination (forward case) and the

#202344 - $15.00 USD Received 2 Dec 2013; revised 20 Jan 2014; accepted 21 Jan 2014; published 3 Feb 2014

noncorrugated-side illumination (backward case) will be carried out in order to confirm the existence and detect the basic features of unidirectional transmission, which is expected to appear in these gratings. Two types of the grating configurations will be studied, which differ from each other in that whether the resulting configuration is single-fraction, i.e., it contains a polar dielectric only, or it is two-fraction, i.e., one of the layers is made of a polar dielectric while the other one is made of a high-ε material to enhance diffraction. A simple approach to the comparison of various polar dielectrics is proposed that allows one selecting a material with a desired width of the ultralow-ε range and, hence, with that of the unidirectional transmission range. The main attention will be paid to the unidirectionality relevant regimes arising due to the common effect of diffraction at the interfaces and dispersion of the polar dielectric. Besides, operation regimes will be studied, which are connected with diffraction only. Calculations are carried out by using an integral equation technique [36].

2. Theoretical background

First, let us consider the general dispersion features of polar dielectrics in the connection with the conditions required for obtaining of unidirectional transmission.

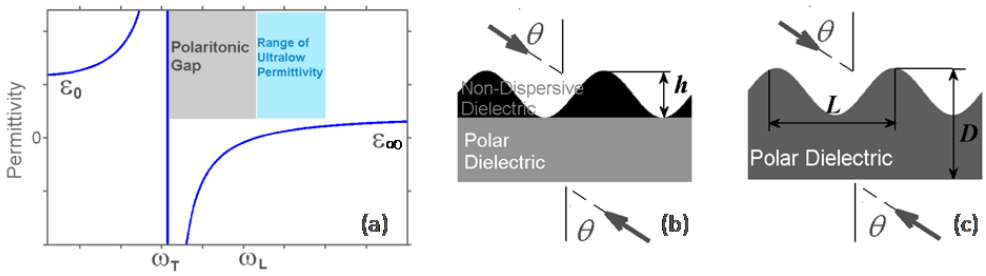

Fig. 1. (a) Typical frequency dependence of permittivity of a polar dielectric ε_P at $\gamma = 0$ and schematics of (b) two-layer and (c) single-layer nonsymmetric gratings containing polar dielectrics; for two- and single-layer gratings, D is the maximal thickness and L is grating period; for two-layer grating, h is thickness of the non-dispersive dielectric layer.

Owing to phonon-photon coupling and polariton excitation, polar dielectrics behave as a strongly dispersive medium whose permittivity depends on frequency as follows [26]:

$$\varepsilon_P(\omega) = \varepsilon_\infty + (\varepsilon_0 - \varepsilon_\infty)\omega_T^2 / (\omega_T^2 - \omega^2 - i\gamma\omega), \quad (1)$$

where ε_0 is the static dielectric constant, ε_∞ is the high-frequency limit of dielectric constant, and γ is the absorption relevant factor. One of the basic features of polar dielectrics is the existence of the polaritonic gap, which corresponds to the range of $\varepsilon_P < 0$, see Fig. 1(a). The frequencies of the lower and upper boundaries of this range are commonly denoted by ω_T and ω_L, respectively. They are connected by the Lyddane-Sachs-Teller relation [25]

$$\omega_L^2 / \omega_T^2 = \varepsilon_0 / \varepsilon_\infty. \quad (2)$$

To obtain dispersion relevant unidirectional transmission, the working frequency range should correspond to $0 < \varepsilon_P < 1$, provided that the surrounding medium is air. One can see in Fig. 1(a) that the corresponding frequency range is located on the right of the polaritonic gap, whereas $\omega = \omega_L$ corresponds to $\varepsilon_P = 0$ for $\gamma = 0$. Clearly, the wider the frequency band, in which $0 < \varepsilon_P < 1$, the wider the range of unidirectional transmission should be. The angular frequency value, at which $\varepsilon_P(\omega)$ achieves a desired value, $\omega = \omega_u$, can easily be obtained

#202344 - $15.00 USD Received 2 Dec 2013; revised 20 Jan 2014; accepted 21 Jan 2014; published 3 Feb 2014

from Eq. (1). For $\varepsilon_P(\omega)=1$ and $\gamma=0$, it yields $\omega_u^2=\left(\varepsilon_\infty\omega_L^2-\omega_T^2\right)/\left(\varepsilon_\infty-1\right)$. Moreover, if the range of $0<\varepsilon_P<1/A$, $A>1$, is considered as the preferable operation range, then

$$\omega_u^2=\left(A\varepsilon_\infty\omega_L^2-\omega_T^2\right)/\left(A\varepsilon_\infty-1\right). \tag{3}$$

Accordingly, the expected width of the range of unidirectional transmission is estimated for given A as

$$\Delta\omega=\omega_u-\omega_L. \tag{4}$$

To compare different polar dielectrics from the point of view of their possible usage for achieving unidirectionality, we introduce the following dimensionless criterium:

$$\zeta=\Delta\omega/\omega_L=\left[\left(A\varepsilon_\infty-\omega_T^2/\omega_L^2\right)/\left(A\varepsilon_\infty-1\right)\right]^{-1/2}-1. \tag{5}$$

It gives the relative width of the frequency band, in which unidirectional transmission is expected to appear. From Eq. (5), it is seen that the stronger the difference between ω_T and ω_L, and the smaller value of ε_∞, the larger ζ is. The values of ω_T, ω_L, ε_0 and ε_∞ can be found in the textbooks [25,37]. However, it is worth noting that these values may differ from one book to another. The values of ω_L/ω_T, ε_∞ and ζ have been compared for various polar dielectrics. Results of the comparison are presented in Table 1, based on the data from Table 3 in Ref [25]. For the sake of definiteness, we take here $A=2$, i.e., $0<\varepsilon_P<0.5$. One can see that there are materials, for which $\omega_L/\omega_T>2$ or/and $\varepsilon_\infty<2$, and thus the values of ζ can be rather large.

Table 1. Comparison of Various Polar Dielectrics in Terms of Characteristics Responsible for the Relative Width of Unidirectional Transmission Range

	ω_L/ω_T	ε_∞	ζ at $A=2$		ω_L/ω_T	ε_∞	ζ at $A=2$
LiH	1.9	3.6	0.057	RbF	1.86	1.9	0.12
LiF	2.07	1.9	0.129	TlCl	2.5	5.1	0.045
LiCl	2.08	2.7	0.084	TlBr	2.35	5.4	0.041
LiBr	2.03	3.2	0.068	AgCl	1.79	4.0	0.048
NaF	1.73	1.7	0.13	MgO	1.87	2.95	0.07
NaCl	1.61	2.25	0.084	GaP	1.1	8.5	0.005
KF	1.69	1.5	0.151	GaAs	1.08	10.9	0.003
KCl	1.48	2.1	0.082	InSb	1.06	15.6	0.002

Clearly, the choice of a certain material depends not only on the values of ω_L/ω_T, ε_∞ and ζ but also on the frequency range targeted. Indeed, the values of ω_T and ω_L substantially differ from one polar dielectric to another, covering a wide frequency range, from units to several tens of terahertz. To better illustrate the possibility of wideband unidirectionality, we selected LiF. According to [27,37], we use $\omega_T=57.98\text{THz}$, $\omega_L=172.22\text{THz}$, $\gamma=4.4\text{THz}$, and $\varepsilon_\infty=1.04$ for this material. Note that these values differ from those given for LiF and promise even a better performance as compared to that based on the data from [25].

In the next section, we consider two configurations, which are referred to as configuration A and configuration B. They are schematically shown in Figs. 1(b) and 1(c), respectively. Configuration A consists of two layers: the noncorrugated layer made of LiF and the corrugated layer made of a dielectric with $\varepsilon_d=5.8$. It is expected that the latter can enhance

#202344 - $15.00 USD Received 2 Dec 2013; revised 20 Jan 2014; accepted 21 Jan 2014; published 3 Feb 2014

transmission, while the former enables directional selectivity at $0 < \varepsilon_P < 1$. The chosen value of ε_d is located in the middle of the range of $5 < \varepsilon_d < 6.5$, to which various dielectrics, e.g., chalcogenide glasses do correspond. For this configuration, we use $D/L = 1.6$ and $h/D = 0.5$. These values and sinusoidal corrugations of the depth of $D - h$ are kept throughout the paper. Configuration B differs from configuration A only in that it is entirely made of LiF. Both configurations are illuminated from either the corrugated or the noncorrugated side at angle θ, which is measured in the counter-clockwise direction from the normal to the illuminated interface.

To characterize asymmetry in transmission and reflection, we use $T^{\rightarrow} = \sum_{(m)} t_m^{\rightarrow}$, $T^{\leftarrow} = \sum_{(m)} t_m^{\leftarrow}$, $R^{\rightarrow} = \sum_{(m)} r_m^{\rightarrow}$, and $R^{\leftarrow} = \sum_{(m)} r_m^{\leftarrow}$, where $T^{\rightarrow}$, $T^{\leftarrow}$, $R^{\rightarrow}$, and $R^{\leftarrow}$ mean corrugated-side (forward) transmittance, noncorrugated-side (backward) transmittance, corrugated-side reflectance, and noncorrugated-side reflectance, respectively, and $t_m^{\rightarrow}$, $t_m^{\leftarrow}$, $r_m^{\rightarrow}$, and $r_m^{\leftarrow}$ mean the corresponding mth -order (partial) transmittances and reflectances. It is noteworthy that $t_0 = t_0^{\rightarrow} = t_0^{\leftarrow}$ because of the Lorentz reciprocity.

According to the general theory of the diffraction inspired unidirectional transmission [38], variation in ε_P can strongly affect the achievable regimes. In particular, the width of the θ range, in which unidirectional transmission is possible, depends on ε_P. As follows from the analysis of coupling for circular equifrequency dispersion contours in [38], the condition

$$\varepsilon_P^{1/2} + 1 > 2\pi/(kL), \tag{6}$$

where $k = \omega/c$, is necessary for obtaining of unidirectional transmission at least within a narrow θ range, at given kL. In turn, this leads to restrictions on the value of A in Eq. (3). If $\varepsilon_P^{1/2} = \pi/(kL) = 1/3$, the range of θ, in which unidirectional transmission is expected to appear, extends from $\theta_1 = \arcsin(1/3)$ to $\theta_2 = \pi/2$ [38].

3. Basic features of transmission and reflection

In Fig. 2, forward transmittance and forward-to-backward transmittance contrast, $C_T = 20\log_{10} T^{\rightarrow}/T^{\leftarrow}$, are presented for the two configurations, which are expected to enable unidirectional transmission. A rather large value of θ has firstly been taken to ensure wideband unidirectionality. In the presented example, $T^{\rightarrow} > 0$, $T^{\leftarrow} \approx 0$ and $C_T > 70$dB at least at $14.4 < kL < 19$. This kL-range corresponds to $28.2\text{THz} < f < 37.2\text{THz}$, whereas $L = 24\mu\text{m}$. In turn, the polaritonic gap extends from $kL \approx 1.5\pi$ to $kL \approx 14$. Owing to the non-dispersive dielectric layer, the two-layer (two-fraction) grating is characterized by higher transmission than the one-layer (one-fraction) grating, but C_T is higher for the latter. This is not a surprising feature, since the ultralow-ε material occupies a larger volume in this case. In Figs. 2(a) and 2(b), one can see that several diffraction orders contribute to $T^{\rightarrow}$. In line with the grating theory [39], the mth order may propagate in air starting from

$$kL = k_m L = 2\pi |m|/(1 - \operatorname{sgn} m \sin\theta). \tag{7}$$

In Fig. 2(a), the order $m = -2$ appears first, so that $T^{\rightarrow} \approx t_{-2}^{\rightarrow}$ in the vicinity of $kL = 15$. Then, the orders $m = -3$, $m = -1$, and $m = -4$ appear at $kL \approx 15.2$, $kL \approx 16.2$, and $kL \approx 17.1$,

#202344 - $15.00 USD Received 2 Dec 2013; revised 20 Jan 2014; accepted 21 Jan 2014; published 3 Feb 2014

respectively. Thus, the conventional order in appearance of higher orders that corresponds to Eq. (6) is broken here. In Fig. 2(b), $T^{\rightarrow} \approx t^{\rightarrow}_{-2}$ up to $kL \approx 16$, where the orders $m = -1$ and $m = -3$ start contributing to $T^{\rightarrow}$. Since transmission is entirely suppressed within the considered kL-range at the noncorrugated-side illumination [see Fig. 2(c)], asymmetry in transmission occurs also in the actual mth-order frequency thresholds (wavelength cutoffs), i.e., they differ for the two utilized illumination directions.

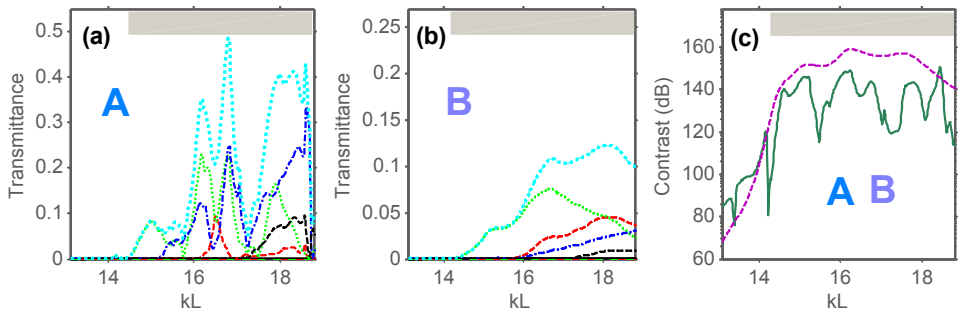

Fig. 2. $T^{\rightarrow}$ and $t^{\rightarrow}_{m}$ vs kL for configurations (a) A and (b) B, and (c) C_T vs kL, at $\omega_T L / c = 1.5\pi$ and $\theta = 60°$; (a) and (b): $t^{\rightarrow}_{m}$ at $m = -1$ - red dashed line, $m = -2$ - green dotted line, $m = -3$ - blue dash-dotted line, $m = -4$ - black dashed line, and $T^{\rightarrow}$ - cyan dotted line; (c): C_T for configurations A and B is shown by dark-green solid line and violet dashed line, respectively; gray rectangles - locations of the unidirectional transmission ranges.

On the contrary to Fig. 2, there is no anomaly in threshold frequencies (cutoff wavelengths), starting from (up to) which $r^{\rightarrow}_{m}$ contributes to $R^{\rightarrow}$. At the same time, $R^{\leftarrow} \approx r_0 > 0.9$ in the considered kL-range, for the both configurations A and B. Hence, reflections are not affected by the corrugations of the exit interface, i.e., the grating behaves in the reflection regime similarly to a noncorrugated ultralow-ε layer. As a result, strong asymmetry takes place in reflection and, in particular, in the frequency thresholds.

In Fig. 3, the dependencies of $t^{\rightarrow}_{m}$, $T^{\rightarrow}$, and C_T on kL are presented for the same parameter settings as in Fig. 2, but now for smaller values of θ. The effect of decrease of θ is well seen from the comparison of Figs. 2 and 3. In particular, some narrowing of the unidirectional transmission range, weaker difference between configurations A and B in terms of $\max T^{\rightarrow}$, and increase of $T^{\rightarrow}$ for configuration B should be noticed. For the values of θ used in Fig. 3, unidirectionality is still a wideband effect. For a larger part of the unidirectional transmission range, higher contrasts are observed for configuration B. For instance, this takes place at $kL = 16.2$ in Fig. 3(c), where $T^{\rightarrow} \approx t^{\rightarrow}_{-1} + t^{\rightarrow}_{-2} \approx 0.2$ and $C_T = 120\text{dB}$. Hence, directional selectivity can occur in a wide range of θ variation that enables tunability. Further decrease of θ results in that the order $m = 0$ is coupled at smaller values of kL than in Fig. 3, in accordance with the general theory of the diffraction inspired unidirectional transmission [38]. This leads to that the unidirectionality disappears, provided that the coupling for zero order is not vanishingly weak.

#202344 - $15.00 USD Received 2 Dec 2013; revised 20 Jan 2014; accepted 21 Jan 2014; published 3 Feb 2014

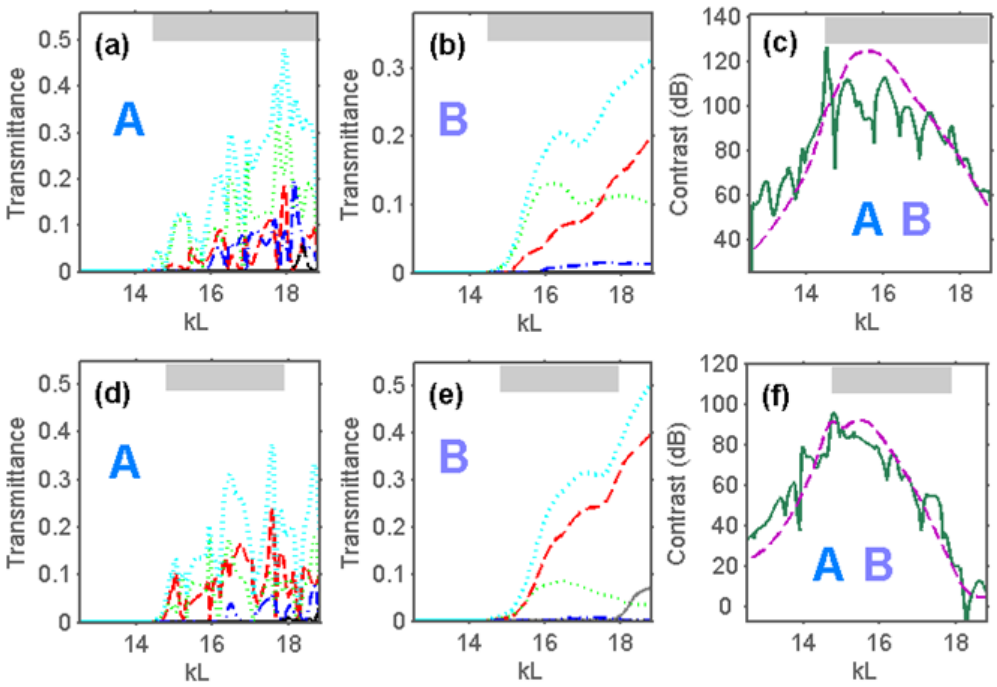

Fig. 3. $T^{\rightarrow}$ and $t_m^{\rightarrow}$ vs kL for configurations (a,d) A and (b,e) B, and (c,f) C_T vs kL, at $\omega_T L/c = 1.5\pi$, (a-c) $\theta = 47°$ and (d-f) $\theta = 40°$; (a), (b), (d), (e): $t_m^{\rightarrow}$ at $m = 0$ - gray solid line, $m = -1$ - red dashed line, $m = -2$ - green dotted line, $m = -3$ - blue dash-dotted line, $m = -4$ - black dashed line, and $T^{\rightarrow}$ - cyan dotted line; (c,f): C_T for configurations A and B is shown by dark-green solid line and violet dashed line, respectively; gray rectangles - unidirectional transmission ranges.

4. Decreasing grating period and thickness

Now let us consider the basic effects arising due to decrease of $\omega_T L/c$ at fixed other parameters. In fact, this means that we take a smaller value of L, and – since D/L is assumed to be fixed – also a smaller value of D. Shift of the unidirectional transmission range towards smaller values of kL, significant single-beam transmission due to lower nonzero diffraction orders, and change of the sequence in appearance of higher orders are among the expected effects. First, we take $\omega_T L/c = 1.1\pi$ that corresponds to the polaritonic gap ranging from $kL = 1.1\pi$ to $kL = 10.4$ and $L = 17.9\mu\text{m}$. In Fig. 4, an example of the dependencies of $t_m^{\rightarrow}$ and $T^{\rightarrow}$ on kL is presented at the same parameters as in Fig. 2, except of the value of $\omega_T L/c$. Comparing to Fig. 2, stronger forward transmission can be obtained for configuration A in the unidirectional regime. Thus, at large values of θ, a proper choice of $\omega_T L/c$ can help to enhance performance for the two-layer (two-fraction) grating. At the same time, forward transmission for configuration B has not been substantially enhanced.

#202344 - $15.00 USD Received 2 Dec 2013; revised 20 Jan 2014; accepted 21 Jan 2014; published 3 Feb 2014

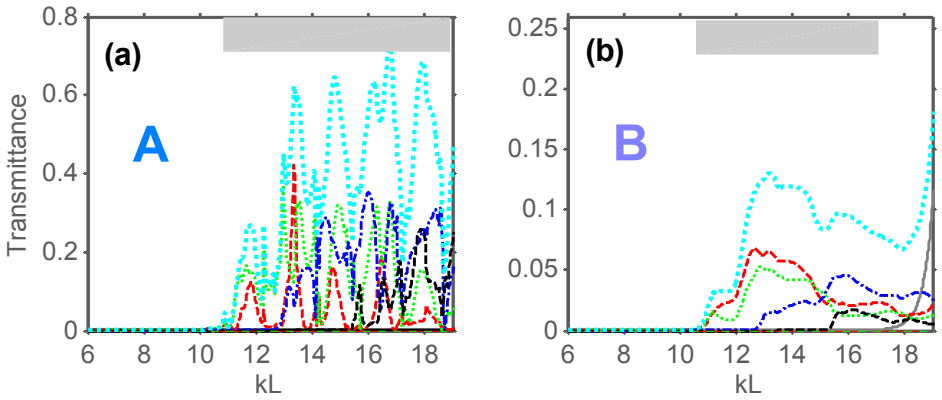

Fig. 4. $T^{\rightarrow}$ and $t_m^{\rightarrow}$ vs kL for configurations (a) A and (b) B at $\omega_T L / c = 1.1\pi$ and $\theta = 60°$; $t_m^{\rightarrow}$ at $m = 0$ - gray solid line, $m = -1$ - red dashed line, $m = -2$ - green dotted line, $m = -3$ - blue dash-dotted line, $m = -4$ - black dashed line, and $T^{\rightarrow}$ - cyan dotted line; gray rectangles - unidirectional transmission ranges.

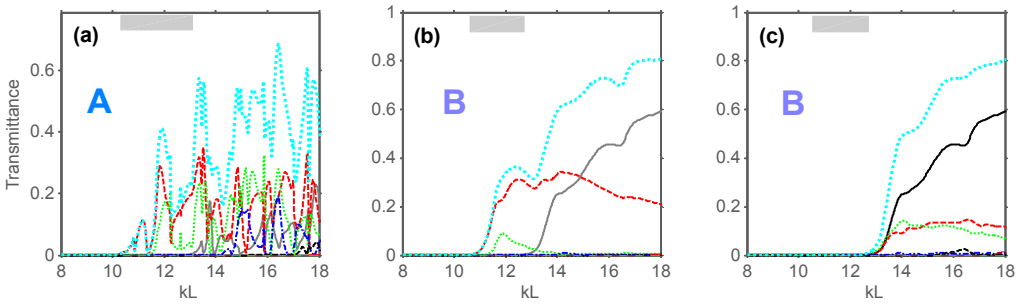

Fig. 5. $T^{\rightarrow}$ and $t_m^{\rightarrow}$ for configurations (a) A and (b) B, and (c) $T^{\leftarrow}$ and $t_m^{\leftarrow}$ for configuration B at $\omega_T L / c = 1.1\pi$ and $\theta = 40°$; $t_m^{\rightarrow}$ and $t_m^{\leftarrow}$ at $m = 0$ - gray solid line, $m = -1$ - red dashed line, $m = -2$ - green dotted line, $m = -3$ - blue dash-dotted line, $m = -4$ - black dashed line, $T^{\rightarrow}$ and $T^{\leftarrow}$ - cyan dotted line; gray rectangles - unidirectional transmission ranges.

To compare, Fig. 5 presents the results for a smaller value of θ. In turn, Figs. 5(a) and 5(b) differ from Figs. 3(d) and 3(e) only in the value of $\omega_T L / c$. The basic features relevant to the θ variation are similar to those observed at $\omega_T L / c = 1.5\pi$. However, the narrowing of the unidirectional range, which is inspired by decrease of θ, is now much stronger pronounced. Comparing Figs. 5(b) and 5(c), one can see that unidirectional transmission with $T^{\rightarrow} \approx t_{-1}^{\rightarrow}$, $\max t_{-1}^{\rightarrow} \approx 0.31$ and $T^{\leftarrow} \approx 0$ is obtained in the vicinity of $kL = 12.5$. Hence, wideband unidirectionality with a rather high $T^{\rightarrow}$ can also be obtained for configuration B, i.e., when using a single-layer grating, at least at intermediate θ.

#202344 - $15.00 USD Received 2 Dec 2013; revised 20 Jan 2014; accepted 21 Jan 2014; published 3 Feb 2014

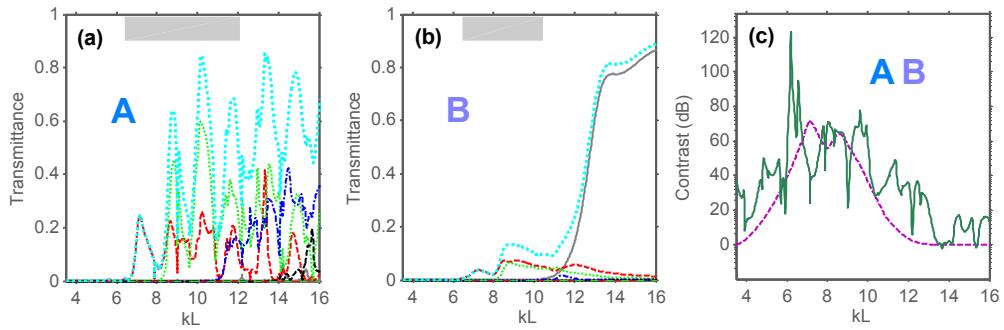

Fig. 6. Same as Fig. 2 but for $\omega_T L / c = 0.7\pi$; (a,b) gray solid line - t_0 .

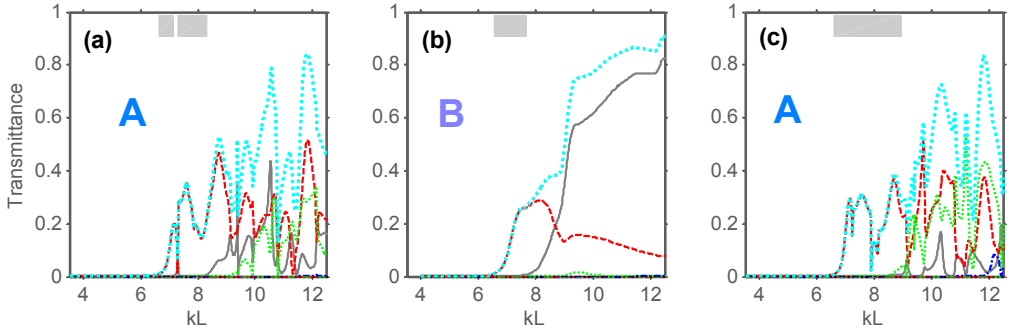

Fig. 7. $T^{\rightarrow}$ and $t_m^{\rightarrow}$ for configuration (a) A at $\theta = 40°$, (b) configuration B at $\theta = 40°$, and (c) configuration A at $\theta = 47°$, when $\omega_T L / c = 0.7\pi$; $t_m^{\rightarrow}$ at $m = 0$ - gray solid line, $m = -1$ - red dashed line, $m = -2$ - green dotted line, $m = -3$ - blue dash-dotted line, and $T^{\rightarrow}$ - cyan dotted line; gray rectangles - unidirectional transmission ranges.

Next, we further decrease $\omega_T L / c$. In Fig. 6, $t_m^{\rightarrow}$, $T^{\rightarrow}$ and C_T vs kL are presented at $\omega_T L / c = 0.7\pi$ and $\theta = 60°$. Now, the polaritonic gap corresponds to $0.7\pi < kL < 6.61$ and $L = 11.4\mu\text{m}$. For configuration A, $T^{\rightarrow}$ in the unidirectional regime is further enhanced. For configuration B, it remains low. Hence, at large θ , such a decrease of $\omega_T L / c$ has sense only for configuration A. It is noteworthy that larger values of $T^{\rightarrow}$ in Fig. 6(a) are achieved at the price of decrease of C_T , as follows from the comparison of Figs. 6(c) and 2(c). Moreover, C_T decreases for configuration B, too. In the contrast with Fig. 2(c), C_T is now higher for configuration A, over a larger part of the unidirectional transmission range. Asymmetry in reflection is also observed in this case. It manifests itself in the similar way as described above, e.g., $R^{\leftarrow} \approx r_0$ within a wide frequency range. For the sake of completeness, we consider diffraction at smaller values of θ and the same $\omega_T L / c$ as in Fig. 6. Results are presented in Figs. 7 and 8. Single-beam unidirectional transmission with $T^{\rightarrow} \approx t_{-1}^{\rightarrow}$ is observed at $6.2 < kL < 7.1$ and $7.35 < kL < 8.25$ in Fig. 7(a), at $6.5 < kL < 7.5$ in Fig. 7(b), and at $6.5 < kL < 8.5$ in Fig. 7(c). To further increase $\max T^{\rightarrow}$, additional optimization is required.

#202344 - $15.00 USD Received 2 Dec 2013; revised 20 Jan 2014; accepted 21 Jan 2014; published 3 Feb 2014

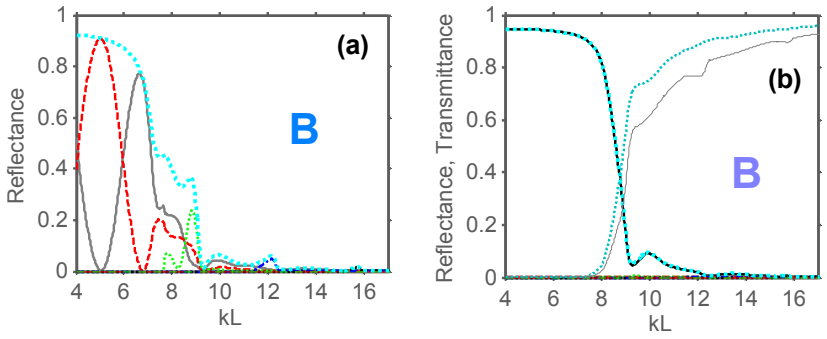

Fig. 8. $R^{\rightarrow}$ and $r_m^{\rightarrow}$ (a) and $R^{\leftarrow}$ and $r_m^{\leftarrow}$ (b) vs kL for configuration B at $\omega_T L/c = 0.7\pi$ and $\theta = 40°$; $r_m^{\rightarrow}$ and $r_m^{\leftarrow}$ at $m = 0$ - gray solid line, $m = -1$ - red dashed line, $m = -2$ - green dotted line, $m = -3$ - blue dash-dotted line, $R^{\rightarrow}$ and $R^{\leftarrow}$ - cyan dotted line; (b): t_0 and $T^{\leftarrow}$ are shown by thin gray solid line and thin cyan dotted line, respectively.

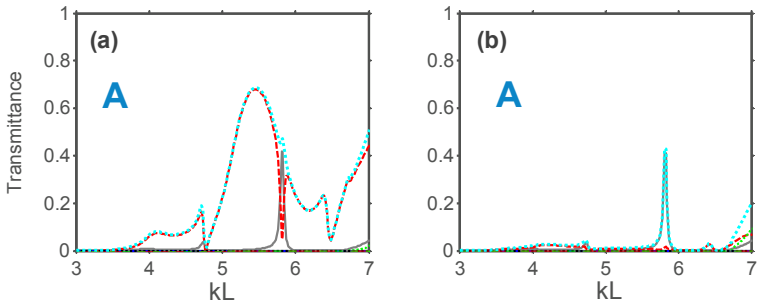

Fig. 9. $T^{\rightarrow}$ and $t_m^{\rightarrow}$ (a) and $T^{\leftarrow}$ and $t_m^{\leftarrow}$ (b) for configuration A at $\omega_T L/c = 0.4\pi$ and $\theta = 60°$, and same other parameters and notations as in Fig. 5.

In Fig. 8, $r_m^{\rightarrow}$, $r_m^{\leftarrow}$, $R^{\rightarrow}$ and $R^{\leftarrow}$ vs kL are shown for the same case as in Fig. 7(b) and for the corresponding case of noncorrugated-side illumination. Besides, t_0 and $T^{\leftarrow}$ are presented in Fig. 8(b). One can see that the contribution of $r_m^{\rightarrow}$ to $R^{\rightarrow}$ strongly differs from that of $r_m^{\leftarrow}$ to $R^{\leftarrow}$. In particular, $R^{\leftarrow} \approx r_0$ over a wide kL-range, while all of the orders $m = 0, -1, -2, -3$ contribute to $R^{\rightarrow}$. At $kL > 12$, there are no significant reflections. At the same time, most part of the incident-wave energy can be converted into a reflected higher-order beam, as occurs in Fig. 8(a) at $kL = 5$. A quite strong asymmetry in transmission can be possible even at smaller values of L and $\omega_T L/c$ than in Figs. 2-8. As an example, Fig. 9 presents the results for $\omega_T L/c = 0.4\pi$. Unidirectional transmission is observed in this case with $\max T^{\rightarrow} \approx \max t_{-1}^{\rightarrow} > 0.6$ and $T^{\leftarrow} \approx 0$ near $kL = 5.4$. It is worth noting that the polaritonic gap is located here at $0.4\pi < kL < 3.78$ where $L \approx 6.5\mu\text{m}$.

For the comparison purposes, Fig. 10 presents the results for the grating, which differs from configuration A in that the ultralow-ε layer is made of NaCl. For this material, $\omega_T = 30.9\text{THz}$, $\omega_L = 50.37\text{THz}$, $\gamma = 1.2\text{THz}$, and $\varepsilon_\infty = 2.22$ [27,37]. In this case, the polaritonic gap extends from $kL = 2\pi$ up to $kL \approx 10.2$ and $L = 61\mu\text{m}$. The range of unidirectional transmission is located at $10.4 < kL < 12$ that approximately corresponds to

#202344 - $15.00 USD Received 2 Dec 2013; revised 20 Jan 2014; accepted 21 Jan 2014; published 3 Feb 2014

$8.15\text{THz} < f < 9.4\text{THz}$. As expected, this range is narrower than for LiF, because of smaller ω_L / ω_T and larger ε_∞. In spite of this, NaCl can be a reasonable choice when a lower frequency range is targeted.

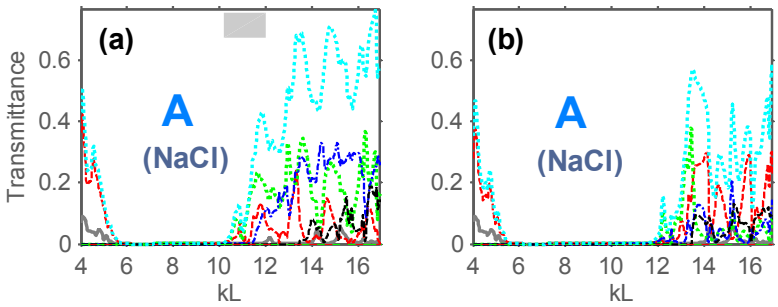

Fig. 10. $T^{\rightarrow}$ and $t_m^{\rightarrow}$ (a) and $T^{\leftarrow}$ and $t_m^{\leftarrow}$ (b) vs kL for a similar configuration as A but with the ultralow-ε layer made of NaCl, at $\omega_T L / c = 2\pi$ and $\theta = 60°$; $t_m^{\rightarrow}$ and $t_m^{\leftarrow}$ at $m = 0$ - gray solid line, $m = -1$ - red dashed line, $m = -2$ - green dotted line, $m = -3$ - blue dash-dotted line, $m = -4$ - black dashed line; $T^{\rightarrow}$ and $T^{\leftarrow}$ - cyan dotted line; gray rectangle - unidirectional transmission range.

5. Dispersion irrelevant asymmetry in transmission

Up to now, we considered asymmetric wave transmission connected with the common effect of dispersion and diffraction at inclined incidence. As known from the earlier works, asymmetry due to the common effect can be quite strong also at normal incidence [3,20]. In particular, it might occur in the gratings based on photonic crystals or materials with hyperbolic type dispersion. However, this regime cannot be obtained in the non-structured configurations based on polar dielectrics, for which asymmetric wave transmission is associated with ultralow ε and, thus, with non-hyperbolic type of dispersion. On the other hand, recent studies show that asymmetry in transmission can be strongly pronounced, even if dispersion is not hyperbolic, i.e., it does not force zero order to be uncoupled [12,21]. Thus, it can be a fully diffraction effect. Furthermore, in this case, stronger transmission often appears at the noncorrugated-side illumination, on the contrary to the above-considered examples. Similar regimes have already been studied in the nonsymmetric dielectric photonic crystal gratings at $\theta = 0$ [12] and $\theta > 0$ [21]. Dependencies of $t_m^{\rightarrow}$, $t_m^{\leftarrow}$, $T^{\rightarrow}$, $T^{\leftarrow}$, and C_T on kL are presented in Fig. 11, for the same configurations as in Figs. 2 and 3 but for $\theta = 0$. One can see that a well pronounced contrast can be achieved within several narrow frequency ranges for configuration A, whereas asymmetry in transmission is weakly pronounced for the corresponding configuration B. For example, this situation occurs at $kL = 16.5$, i.e., for one of the dips of $C_T < -20\text{dB}$ in Fig. 11(c), where $T^{\leftarrow} = 0.4$ and $t_{-1}^{\leftarrow} = 0.18$. It is expected that this regime of asymmetric wave transmission can be obtained for various polar dielectrics, including those with a narrow range of ultralow ε, see Table 1. Indeed, if it is not necessary that zero order is formally uncoupled, the requirement of a wide range of $0 < \varepsilon_P < 1/A$, $A > 1$ can be cancelled. Thus, more polar dielectrics can be considered as viable candidates to design gratings that are similar to the configurations A and B. In Fig. 12, an example of the dependencies of $t_m^{\rightarrow}$, $t_m^{\leftarrow}$, $T^{\rightarrow}$, $T^{\leftarrow}$, and C_T on kL is presented for the grating that differs from configuration B only in the used polar dielectric. Here, it is GaAs, which has $\omega_T = 8.12\text{THz}$, $\omega_L = 8.75\text{THz}$, $\gamma = 0.5\text{THz}$, and $\varepsilon_\infty = 10.9$ [26].

#202344 - $15.00 USD Received 2 Dec 2013; revised 20 Jan 2014; accepted 21 Jan 2014; published 3 Feb 2014

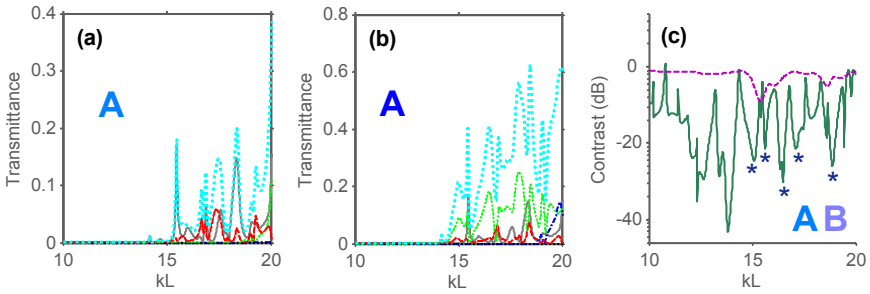

Fig. 11. $T^{\rightarrow}$ and $t_m^{\rightarrow}$ vs kL for configuration A (a), $T^{\leftarrow}$ and $t_m^{\leftarrow}$ for configuration A (b), and C_T for configurations A and B (c), at $\omega_T L / c = 1.5\pi$ and $\theta = 0$; (a) and (b): $t_m^{\rightarrow}$ and $t_m^{\leftarrow}$ at $m = 0$ - gray solid line, $m = \pm 1$ - red dashed line, $m = \pm 2$ - green dotted line, $m = \pm 3$ - blue dash-dotted line, and $T^{\rightarrow}$ and $T^{\leftarrow}$ - cyan dotted line; (c): C_T for configurations A and B is shown by dark-green solid line and violet dashed line, respectively; asterisks indicate the cases of $C_T < -20\text{dB}$.

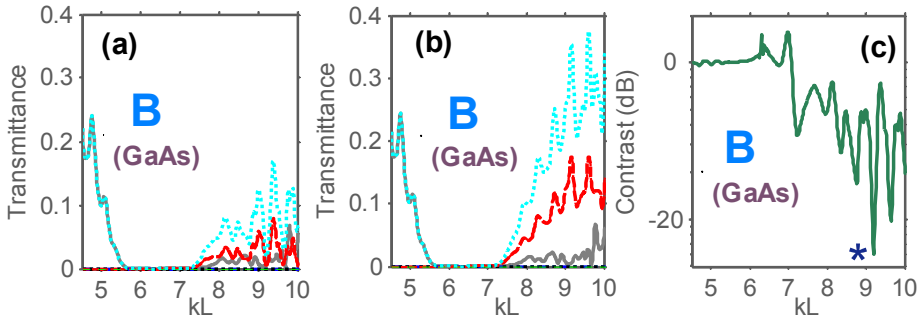

Fig. 12. $T^{\rightarrow}$ and $t_m^{\rightarrow}$ (a), $T^{\leftarrow}$ and $t_m^{\leftarrow}$ (b), and C_T (c) vs kL, for configuration that is similar to B but made of GaAs, at $\omega_T L / c = 2\pi$ and $\theta = 0$; (a) and (b): $t_m^{\rightarrow}$ and $t_m^{\leftarrow}$ at $m = 0$ - gray solid line, $m = \pm 1$ - red dashed line, and $T^{\rightarrow}$ and $T^{\leftarrow}$ - cyan dotted line; (c): asterisk indicates the case of $C_T < -20\text{dB}$.

At the chosen value of $\omega_T L / c$, the polaritonic gap is located at $2\pi < kL < 6.77$. Since $\omega_L / \omega_T \approx 1.08$ and ε_∞ is rather large, wideband unidirectional transmission due to the common effect of dispersion and diffraction is not expected to appear. However, as seen in Fig. 12, asymmetry in transmission can be quite strong within a narrow range near $kL = 9.2$, where $T^{\rightarrow} \approx t_{-1}^{\rightarrow} + t_{+1}^{\rightarrow} > 0.3$. Hence, neither large ω_L / ω_T nor small ε_∞ is necessary for obtaining of a strongly pronounced asymmetry.

6. Conclusions

Merging the recently developed asymmetric wave transmission theory with the peculiar dispersion of polar dielectrics creates a proper platform to realize wideband directional selectivity at terahertz frequencies. In spite of that nonreciprocal operation regimes cannot be achieved in this framework because additional transmission channels (higher orders in our case) are needed to accept the re-directed energy, it looks very promising for manipulation of terahertz waves. Based on the obtained results, the main features of asymmetry arising in transmission and reflection have been demonstrated for the nonsymmetric gratings, which

#202344 - $15.00 USD Received 2 Dec 2013; revised 20 Jan 2014; accepted 21 Jan 2014; published 3 Feb 2014

contain polar dielectrics working in the ultralow-ε regime inspired by phonon-photon coupling. The best pronounced asymmetry results from the common effect of asymmetric coupling and diffractions at the two interfaces, on the one hand, and the ultralow-ε relevant dispersion features, on the other hand. It can be obtained at large and intermediate angles of incidence. Adding a high-ε corrugated layer is required for obtaining of significant transmission at large angles, while both single-fraction and two-fraction nonsymmetric grating can be used at intermediate angles. However, transmission can be quite strong for one of the two incidence directions and can vanish for the opposite direction, even if dispersion does not force zero order, which is responsible for the symmetric transmission component, to be uncoupled. This regime is especially important for small angles, at which the common effect based mechanism is not possible. It can be achieved both with and without the use of the high-ε corrugated layer, depending on the chosen material and geometrical parameters. Hence, co-existence of dispersion relevant and irrelevant unidirectional regimes is not a unique feature of more complex nonsymmetric structures, e.g., photonic crystal gratings. The main regimes of such structured configurations can be replicated in simpler configurations but optimization can be required in order to achieve high transmittance for one of the two directions. Although only two types of simple nonsymmetric gratings have been considered here, more advanced structures could be suggested that exploit the same mechanism. Adjustment of thickness-to-period ratio allow us controlling contribution of desired and unwanted diffraction orders within the unidirectional range.

Acknowledgments

This work is supported by the projects DPT-HAMIT, ESF-EPIGRAT, NATO-SET-181, and by TUBITAK under Project Nos., 107A004, 109A015, 109E301. Contribution of A.E.S. has partially been supported by the Matsumae International Foundation (MIF), Japan under Research Fellowship Program. E.O. acknowledges partial support from the Turkish Academy of Sciences.

#202344 - $15.00 USD Received 2 Dec 2013; revised 20 Jan 2014; accepted 21 Jan 2014; published 3 Feb 2014